ELSEVIER

Surface Science 507–510 (2002) 305–310

SURFACE SCIENCE

www.elsevier.com/locate/susc

Meandering instability of curved step edges on growth of a crystalline cone

M. Rusanen [a,b,*], I.T. Koponen [b], T. Ala-Nissila [a,c]

[a] *Helsinki Institute of Physics and Laboratory of Physics, Helsinki University of Technology, P.O. Box 1100, FIN-02015 HUT, Espoo, Finland*

[b] *Department of Physics, University of Helsinki, P.O. Box 64, FIN-00014 Helsinki, Finland*

[c] *Department of Physics, Brown University, Providence, RI 02912–1843, USA*

Abstract

We study the meandering instability during growth of an isolated nanostructure, a crystalline cone, consisting of concentric circular steps. The onset of the instability is studied analytically within the framework of the standard Burton–Cabrera–Frank model, which is applied to describe step flow growth in circular geometry. We derive the correction to the most unstable wavelength and show that in general it depends on the curvature in a complicated way. Only in the asymptotic limit where the curvature approaches zero the results are shown to reduce to the rectangular case. The results obtained here are of importance in estimating growth regimes for stable nanostructures against step meandering. © 2002 Elsevier Science B.V. All rights reserved.

Keywords: Growth; Surface diffusion; Models of surface kinetics

1. Introduction

Film growth by molecular beam epitaxy (MBE) is essentially based on the possibility to control growth on a submonolayer level. Usually one aims at surfaces as smooth as possible with atomistically sharp structures consisting of step edges or nanoscale islands. Growth of these structures in MBE is affected not only by stochastic but also by deterministic instabilities such as step meandering and bunching. Since the advent of modern film growth techniques these surface instabilities have been of theoretical and practical interest [1,2].

To obtain nanostructures in MBE with desired quality one of the fundamental concerns is the stability of step edges. Instabilities lead to non-uniform layers so it is advantageous to suppress them during growth. In step flow growth the basic mechanism and properties of the meandering instability were explained by Bales and Zangwill (BZ) [3] on the basis of the classic Burton–Cabrera–Frank (BCF) model [4] and the Mullins-Sekerka instability [5]. The case of circular nanostructures has so far received much less attention although it is an example for a layered nanostructure [6]. Decay of mesoscopic circular stepped structures can be described in some special cases of stable step flow with good accuracy using the BCF model [1,6]. Also, recently the decay and bunching

* Corresponding author. Address: Helsinki Institute of Physics, University of Helsinki, P.O. Box 9, 00014 Helsinki, Finland. Tel.: +358-9-451-5806; fax: +358-9-451-2177/+358-9-191-8458.

E-mail address: marko.rusanen@hut.fi (M. Rusanen).

0039-6028/02/$ - see front matter
PII: S0039-6028(02)01262-1

of a circular crystalline cone in the stable growth regime has been studied in detail using a similar approach [7]. However, to our knowledge there has been no study of the meandering instability in the spirit of BZ during growth of circular nanostructures even though its importance was noted already a decade ago [3]. It is thus of interest to know under which conditions circular step edges are stable against meandering. In this report we present our study of the morphological instability of curved step edges. Our viewpoint is based on the BCF model and we generalize the BZ results to the case of a circular geometry. We perform a linear stability analysis and calculate the corrections to the results for the straight steps. As expected, our results reduce to the BZ case in the limit of an infinite step radius.

2. Step flow growth in circular geometry

We study a model of circular steps which are placed concentrically on top of each other. The steps can absorb and emit atoms which diffuse on terraces between the steps. The terrace j is bounded by the steps at r_j and r_{j+1}. Assuming the flux of adatoms onto and evaporation from the terraces, the adatom concentration c_j on the terrace j obeys the well-known form of the BCF equation [3,4].

$$\frac{\partial c_j}{\partial t} = D_s \nabla^2 c_j - c_j/\tau + F, \tag{1}$$

where D_s is the diffusion coefficient of an adatom on a flat terrace; τ, the time scale for evaporation; and F, the deposition flux. Assuming that the adatom concentration relaxes much faster than the step edge moves we can assume that the terrace is in a quasi-stationary state corresponding to $\partial c_j/\partial t = 0$. Mass transport through the bulk of the material is ignored.

The model is now fully specified with the choice of the boundary conditions and the requirement of the mass conservation at the step edges. The mass conservation implies that the edge velocity is given by [3]

$$V_j = V_{j+} + V_{j-} = \Omega D_s \left(\left.\frac{\partial c_j}{\partial r}\right|_{R_j} - \left.\frac{\partial c_{j-1}}{\partial r}\right|_{R_j} \right), \tag{2}$$

where Ω is the atomic area; V_{j-}, V_{j+}, the contributions to the step edge velocity due to surface currents from the upper and lower terrace, respectively; and R_j, the radius of the jth step edge. We assume that the velocities $V_{j\mp}$ are related to the deviations of the adatom concentration from the equilibrium value [8]

$$V_{j\pm} = \Omega k_{\pm} \left[c_j - c_j^{\mathrm{eq}} \right], \tag{3}$$

where $c_j^{\mathrm{eq}} = c_0^{\mathrm{eq}} \exp[\tilde{\Gamma}\kappa(R_j)]$ is the equilibrium adatom concentration at the edge, $\tilde{\Gamma} = \Omega\gamma/(k_B T)$; γ, the free energy/(unit length); c_0^{eq}, the equilibrium adatom concentration at the straight step; and $\kappa(R_j)$, the local curvature of the step in the circular geometry [9]. The attachment coefficients k_-, k_+ associated with the upper and lower terraces, respectively, can be related to the Ehrlich–Schwoebel barrier [10] at the step edge [11]. From Eqs. (2) and (3) we obtain the mixed boundary conditions at the step edge

$$\begin{aligned} D_s \left.\frac{\partial c_j}{\partial r}\right|_{R_j} &= k_+ \left[c_j|_{R_j} - c_j^{\mathrm{eq}} \right], \\ -D_s \left.\frac{\partial c_j}{\partial r}\right|_{R_{j+1}} &= k_- \left[c_j|_{R_{j+1}} - c_{j+1}^{\mathrm{eq}} \right]. \end{aligned} \tag{4}$$

Defining a new field $u_j = c_i - \tau F$ Eq. (1) becomes the Helmholtz equation in the stationary limit [3,4]:

$$\nabla^2 u_j - \frac{1}{x_s^2} u_j = 0, \tag{5}$$

where $x_s = (D_s\tau)^{1/2}$ is the diffusion length. The solution of Eq. (5) for the perfectly circular step is given by $u_j^0(r) = a_j^0 I_0(r/x_s) + b_j^0 K_0(r/x_s)$, where $I_0(x)$ and $K_0(x)$ are the zeroth order modified Bessel functions [12] and a_j^0 and b_j^0 are coefficients determined by the boundary conditions. In the linear stability analysis a small perturbation is added to the step edge and the equations are solved to first order in the perturbation amplitude. We set $\tilde{r}_j(\theta) = R_j + \epsilon \exp[in\theta + \omega t] + \text{c.c.}$, where ϵ is a small parameter, ω a growth rate, $|n| \geqslant 1$ is an integer (due to periodicity), and c.c. denotes the complex conjugate. The solution to Eq. (5) in the first order in ϵ gives $u_j(r,\theta) = u_j^0(r) + \epsilon[A_j^n I_n(r/x_s) + B_j^n K_n(r/x_s)] \exp(in\theta + \omega t)$, where $K_n(x)$ and $I_n(x)$ are the modified Bessel functions of integer order

n, and the coefficients A_j^n and B_j^n are determined by the boundary conditions. When the solution is found, the growth rate ω can be deduced using Eq. (2) and $V_j = V_j^0 + \omega\tilde{r}_j(\theta)$. If $\omega > 0$, the step edge is linearly unstable.

For simplicity we have not included the step permeability [13] to the model which would be important e.g. in the case of a decaying cone [14]. The step permeability would enhance the downward mass currents and possibly make the steps more stable against meandering. The generalization of this work to permeable steps is straightforward.

3. Morphological instability of a circular step

Qualitatively, the growth of stepped structures is unstable against step meandering when the flux of adatoms from the upper terrace is reduced, e.g. due to the Ehrlich–Schwoebel barrier [10]. This is basically the origin of the morphological instability on vicinal surfaces (the BZ case) [3,5]. However, in the case of a circular step, the stabilizing effect of the step curvature is expected to be more pronounced than in the rectangular geometry. Therefore, we expect the possible instability to be weaker than in the rectangular case since the line tension tends to smooth the steps. Here we consider the cases $k_+ \to \infty$, $k_- = 0$ (one-sided model), and $k_+ \neq k_-$ non-zero and finite (asymmetric model).

3.1. One-sided model

In the one-sided model $k_+ \to \infty$ corresponds to instantaneous attachment from the lower terrace and $k_- = 0$ implies an infinite Ehrlich–Schwoebel barrier. In this limit the velocity of the step with radius R is given by $V = V_+ = D\Omega(\partial u/\partial r)$ and the stability function becomes

$$\frac{\omega(n)}{\Omega\Delta F} = \left(\frac{\xi_s}{\rho} - 1\right)\frac{b_n^1 + b_n^2 + b_n^3}{a_n} + c_n\frac{\xi_s}{\rho^2}(1 - n^2), \tag{6}$$

where $\xi_s = \tilde{\Gamma}/(x_s\tau\Delta F)$ is the capillary length, $\Delta F = F - c_0^{eq}\tau$, and $\rho = R/x_s$. The coefficients are given by $a_n = [\widehat{I'_n}K_n - I_n\widehat{K'_n}][\widehat{I_1}K_0 + I_0\widehat{K_1}]$, $b_n^1 = [\widehat{I'_n}K_n - I_n\widehat{K'_n}][I'_1\widehat{K_1} - \widehat{I_1}K'_1]$, $b_n^2 = [I'_n\widehat{K'_n} - \widehat{I'_n}K'_n][I_1\widehat{K_1} - \widehat{I_1}K_1]$, $b_n^3 = [I_nK'_n - I'_nK_n][\widehat{I'_1}\widehat{K_1} - \widehat{I_1}\widehat{K'_1}]$, and $c_n = [\widehat{I'_n}K_n - I_n\widehat{K'_n}][\widehat{I'_n}K_n - I_n\widehat{K'_n}]$, where $I_n \equiv I_n(\rho)$, $\widehat{I_n} \equiv I_n(\rho + l/x_s)$, $K_n \equiv K_n(\rho)$, $\widehat{K_n} \equiv K_n(\rho + l/x_s)$, l is the terrace width, and the prime indicates the derivative with respect to the scaled variable ρ. By using the asymptotic formulae of the modified Bessel functions for n, R large with $n/R \equiv q = \text{const.}$ [12] the growth rate (6) can be shown to reduce to the result of BZ [3] in the limit $R \to \infty$.

The stability function is plotted in Fig. 1 and it approaches a limiting form when the radius of the step increases (curvature decreases). As can be seen from the figure, there exists a limiting value R_c for the radius such that steps with $R < R_c$ are always stable. For radii $R > R_c$ there exists a critical value of the wave vector q_c such that for $q > q_c$ the edge is stable. The critical wave vector depends on curvature and with increasing curvature q_c decreases, i.e. the critical wavelength where the instability sets in is shifted to larger wavelengths.

In the limit of large n, R we obtain the correction term to the results of BZ of the order of $1/R$ as

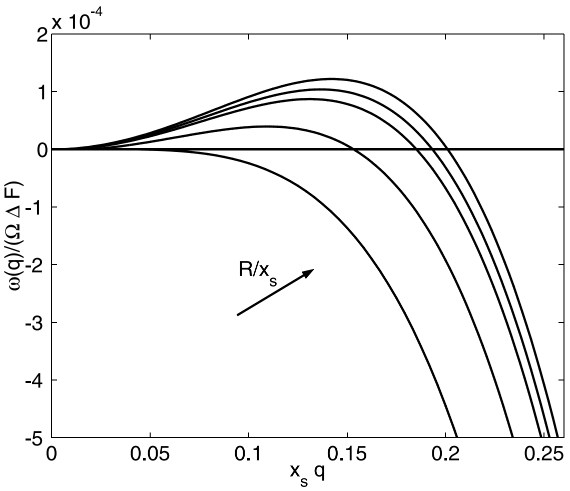

Fig. 1. The growth rate $\omega(q)$ as a function of the wave vector $q = n/R$ with a moderate value of the terrace width l in the case of one-sided model. The stable regime corresponds to $\omega < 0$. The radius of the step R increases in the direction of the arrow. The curves indicate that structures smaller than a critical size R_c are stable against step meandering.

$$\frac{\omega(n)}{\Omega \Delta F} = \omega_{\mathrm{BZ}}(q) + \frac{x_{\mathrm{s}}}{2R}\Sigma_q, \tag{7}$$

where ω_{BZ} is the rectangular result (Eq. (13) in Ref. [13]),

$$\begin{aligned}\Sigma_q = &-\tanh(\tilde{l})(2 + l^2q^2) \\ &+ (l^2q^2 + \Lambda_q^{-2})\tanh^2(\Lambda_q\tilde{l})\tanh(\tilde{l}) \\ &+ (x_{\mathrm{s}}lq^2\Lambda_q^{-2} + \Lambda_q^{-1}\tanh(\Lambda_q\tilde{l})(l^2q^2 + \Lambda_q^{-2}) \\ &+ \tanh(\tilde{l}) - 2\xi_{\mathrm{s}})\frac{1}{\cosh(\Lambda_q\tilde{l})\cosh(\tilde{l})} + 2\xi_{\mathrm{s}} \\ &+ \xi_{\mathrm{s}}x_{\mathrm{s}}^2l^2q^4 - \xi_{\mathrm{s}}x_{\mathrm{s}}q^2(l^2q^2 + \Lambda_q^{-2})\tanh^2(\Lambda_q\tilde{l}),\end{aligned}$$

$\Lambda_q = (1 + (x_{\mathrm{s}}q)^2)^{1/2}$, and $\tilde{l} = l/x_{\mathrm{s}}$. Using the equation above we can determine analytically the corrections to the critical wave vector defined as $\omega(q_{\mathrm{c}}) = 0$. The results are for $l \gg x_{\mathrm{s}}$:

$$x_{\mathrm{s}}q_{\mathrm{c}} \approx \begin{cases}\sqrt{\frac{1}{\xi_{\mathrm{s}}} + \frac{x_{\mathrm{s}}}{2R}\left(\frac{1}{\xi_{\mathrm{s}}} - 2\right)}, & x_{\mathrm{s}}q_{\mathrm{c}} \gg 1, \\ \sqrt{\frac{4}{3}(1 - 2\xi_{\mathrm{s}}) - \frac{2x_{\mathrm{s}}}{R}}, & x_{\mathrm{s}}q_{\mathrm{c}} \ll 1,\end{cases} \tag{8}$$

and for $l \ll x_{\mathrm{s}}$ (and $l^2q_{\mathrm{c}}^2 \ll 1$):

$$x_{\mathrm{s}}q_{\mathrm{c}} \approx \sqrt{\frac{lx_{\mathrm{s}}}{2\xi_{\mathrm{s}}} - 1 - \frac{l}{R}}. \tag{9}$$

Omitting the $1/R$ terms we obtain the BZ results for the rectangular geometry [3]. From these equations we can determine also R_{c} in the case $q_{\mathrm{c}} = 0$ which corresponds to a maximally unstable case in the large R limit. The expressions are $R_{\mathrm{c}} = 3x_{\mathrm{s}}/(2 - 4\xi_{\mathrm{s}})$, when $x_{\mathrm{s}}q_{\mathrm{c}} \ll 1$ (for $l \ll x_{\mathrm{s}}$), and $R_{\mathrm{c}} = l(lx_{\mathrm{s}}/2\xi_{\mathrm{s}} - 1)^{-1}$ for $l \gg x_{\mathrm{s}}$.

In Fig. 2 the curves for the critical wave vector q_{c} against the capillary length ξ_{s} are shown for $l \gg x_{\mathrm{s}}$, $x_{\mathrm{s}}q_{\mathrm{c}} \ll 1$. The corrected result follows the numerically plotted curve whereas the BZ result deviates considerably. For ξ_{s} large enough the edge is always stable and q_{c} approaches zero. The inset of Fig. 2 shows the case $l \ll x_{\mathrm{s}}$ which behaves in a similar way.

3.2. Asymmetric model

When the kinetic coefficients at the step edge from the lower and upper terrace are both finite

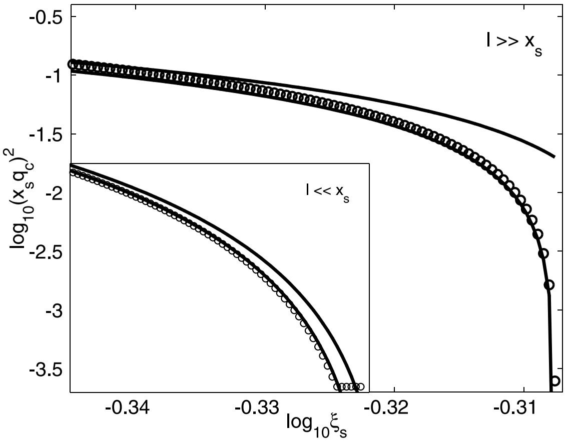

Fig. 2. The critical wave vector q_{c} as a function of the capillary length ξ_{s} in the case of the one-sided model. The circles are Eq. (6), the upper solid line is the BZ result [3], and the lower solid line is Eq. (8) for $l \gg x_{\mathrm{s}}$. The inset shows the case $l \ll x_{\mathrm{s}}$, with the lower solid line given by Eq. (9). The approximations follow the numerically plotted curve, whereas the BZ results deviate for larger values of ξ_{s}.

and non-zero, the velocity of the jth step edge is given by $V_j = D_{\mathrm{s}}\Omega[(\partial u_j/\partial r) - (\partial u_{j-1}/\partial r)]\big|_{r=\tilde{r}_j(\theta)}$ and the growth rate becomes

$$\begin{aligned}\frac{\omega(n,j)}{\Omega\Delta F} = &\left[\frac{\alpha_j}{\gamma_j} - \frac{\alpha_{j-1}}{\gamma_{j-1}}\right]I_0''(\rho_j) + \left[\frac{\beta_j}{\gamma_j} - \frac{\beta_{j-1}}{\gamma_{j-1}}\right]K_0''(\rho_j) \\ &+ \left[\frac{\mathscr{A}_n^j}{\mathscr{D}_n^j} - \frac{\mathscr{A}_n^{j-1}}{\mathscr{D}_n^{j-1}}\right]I_n'(\rho_j) \\ &+ \left[\frac{\mathscr{B}_n^j}{\mathscr{D}_n^j} - \frac{\mathscr{B}_n^{j-1}}{\mathscr{D}_n^{j-1}}\right]K_n'(\rho_j),\end{aligned} \tag{10}$$

where α_j, β_j, and γ_j are the coefficients related to unperturbed steps, and $\mathscr{A}_n^j$, $\mathscr{B}_n^j$, and $\mathscr{D}_n^j$ are obtained from the expansion linear in ϵ. Define $\tilde{d}_\pm = d_\pm/x_{\mathrm{s}} = (D_{\mathrm{s}}/k_\pm)/x_{\mathrm{s}}$, $\mathscr{K}_{n,\pm}^j = K_n(\rho_j) \mp \tilde{d}_\pm K_n'(\rho_j)$ and $\mathscr{I}_{n,\pm}^j = I_n(\rho_j) \mp \tilde{d}_\pm I_n'(\rho_j)$. Then the coefficients are given by

$$\alpha_j = \left(\xi_{\mathrm{s}}/\rho_j - 1\right)\mathscr{K}_{0,-}^{j+1} - \left(\xi_{\mathrm{s}}/\rho_{j+1} - 1\right)\mathscr{K}_{0,+}^j,$$

$$\beta_j = -(\xi_{\mathrm{s}}/\rho_i - 1)\mathscr{I}_{0,-}^{j+1} + \left(\xi_{\mathrm{s}}/\rho_{i+1} - 1\right)\mathscr{I}_{0,+}^j,$$

$$\gamma_j = \mathscr{I}_{0,+}^j\mathscr{K}_{0,-}^{j+1} - \mathscr{I}_{0,-}^{j+1}\mathscr{K}_{0,+}^j,$$

$$\mathscr{A}_n^j = \alpha_j \left[\mathscr{I}_{1,-}^{j+1} \mathscr{K}_{n,+}^j - \mathscr{I}_{1,+}^j \mathscr{K}_{n,-}^{j+1} \right] + \beta_j \left[\mathscr{K}_{1,+}^j \mathscr{K}_{n,-}^{j+1} - \mathscr{K}_{1,-}^{j+1} \mathscr{K}_{n,+}^j \right] - \xi_s (n^2 - 1) \left[\mathscr{K}_{n,+}^j / \rho_{j+1}^2 - \mathscr{K}_{n,-}^{j+1} / \rho_j^2 \right],$$

$$\mathscr{B}_n^j = -\alpha_j \left[\mathscr{I}_{1,-}^{j+1} \mathscr{I}_{n,+}^j - \mathscr{I}_{1,+}^j \mathscr{I}_{n,-}^{j+1} \right] - \beta_j \left[\mathscr{K}_{1,+}^j \mathscr{I}_{n,-}^{j+1} - \mathscr{K}_{1,-}^{j+1} \mathscr{I}_{n,+}^j \right] + \xi_s (n^2 - 1) \left[\mathscr{I}_{n,+}^j / \rho_{j+1}^2 - \mathscr{I}_{n,-}^{j+1} / \rho_j^2 \right],$$

$$\mathscr{D}_n^j = -\mathscr{I}_{n,-}^{j+1} \mathscr{K}_{n,+}^j + \mathscr{I}_{n,+}^j \mathscr{K}_{n,-}^{j+1}.$$

The resulting expression for the growth rate $\omega(q)$ is rather complicated and we have not found any essentially simpler form which would be accurate enough for all curvatures. However, the essential qualitative features can be extracted from the special cases, and the behavior is similar to the one-sided case. The numerically plotted values of ω indicate that as k_- approaches k_+ the growth rate $\omega \leqslant 0$ at all values of q. This is shown in Fig. 3.

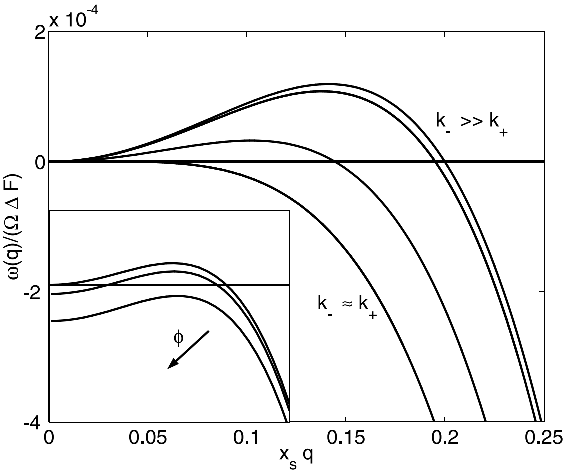

Fig. 3. The instability function $\omega(q)$ as a function of the wave vector q in the asymmetric case. The attachment coefficients k_-, k_+ approach the same value from top to bottom. For $k_- \leqslant k_+$ the steps are always stable. The inset shows ω with increasing phase difference ϕ between two adjacent steps. Increasing ϕ makes steps more stable against meandering as in the rectangular case [15].

We can thus conclude that the one-sided model is the most unstable.

So far, we have only considered the case of in-phase step growth. The stability of growth depends also on the phase of the neighboring steps, and the above analysis can be extended to the more general situation with an arbitrary phase between adjacent steps. However, the general results give only little additional insight and only the numerical results are shown in the inset of Fig. 3. Increasing the phase difference between the two adjacent steps makes the steps more stable as in the case of rectangular geometry [15].

4. Discussion and conclusions

In this work we have generalized the meandering instability to structures made of concentric islands. We have shown that in the case of circular cones growth instability due to terrace diffusion can arise as in the case of rectangular geometry. However, the instability is suppressed by the curvature and structures with smaller sizes than a critical size are stable. The critical size depends on the microscopic parameters of the system. We present here also the asymptotic analytical results for small curvatures. In the limit $R \to \infty$ the growth rate approaches the expression found by BZ [3]. The more general case where attachment from the upper and lower terraces to the step are both finite and non-zero behaves qualitatively similarly to the one-sided model.

The results presented here extend the results of the BZ model for rectangular geometry and they are of interest in modeling e.g. the behavior of isolated crystalline cones. Results given here can be used to check whether the simplified model which assumes the perfectly circular step edges in a decaying cone is valid. If the meandering instability is expected to be present, it can play a significant role in the evolution of nanostructures.

Acknowledgements

We acknowledge the Academy of Finland for financial support, in part through its Center of

Excellence program. M.R. also thanks Magnus Ehrnrooth foundation for travel support.

References

[1] H.-C. Jeong, E.D. Williams, Surf. Sci. Rep. 34 (1999) 171.

[2] P. Politi, G. Grenet, A. Marty, A. Ponchet, J. Villain, Phys. Rep. 324 (1999) 271.

[3] G.S. Bales, A. Zangwill, Phys. Rev. B 41 (1990) 5500, Phys. Rev. B 48 (1993) 2024.

[4] W.K. Burton, N. Cabrera, F.C. Frank, Philos. Trans. R. Soc. London, Ser. A 243 (1951) 299.

[5] W.W. Mullins, R.F. Sekerka, J. Appl. Phys. 35 (1964) 444.

[6] P. Finnie, Y. Homma, Phys. Rev. Lett. 85 (2000) 3237, Phys. Rev. B 62 (2000) 8313.

[7] N. Israeli, D. Kandel, Phys. Rev. Lett. 80 (1998) 3300, Phys. Rev. B 60 (1999) 5946.

[8] A.A. Chernov, Modern Crystallography III, Springer-Verlag, Berlin, 1984.

[9] S.V. Khare, T.L. Einstein, Phys. Rev. B 54 (1996) 11752; J. Miranda, M. Widom, Physica D 120 (1998) 315.

[10] G. Ehrlich, F.G. Hudda, J. Chem. Phys. 44 (1966) 1039; R.L. Schwoebel, E.J. Shipsey, J. Appl. Phys. 37 (1966) 3682.

[11] D. Kandel, Phys. Rev. Lett. 78 (1997) 499.

[12] M. Abramowitz, I.A. Stegun, Handbook of Mathematical Functions, Dover, 1972.

[13] M. Ozdemir, A. Zangwill, Phys. Rev. B 45 (1992) 3718.

[14] S. Tanaka, N.C. Bartelt, C.C. Umbach, R.M. Tromp, J.M. Blakely, Phys. Rev. Lett. 78 (1997) 3342.

[15] A. Pimpinelli, I. Elkinani, A. Karma, C. Misbah, J. Villain, J. Phys. Cond. Matt. 6 (1994) 2661.